Accepted Manuscript

Synthesis of scutellarein derivatives with antiproliferative activity and selectivity through the intrinsic pathway

Tong Han, Yan Wang, Mingying Wang, Xu Li, Keguang Cheng, Xiang Gao, Zhanlin Li, Jiao Bai, Huiming Hua, Dahong Li

PII: S0223-5234(18)30819-5

DOI: 10.1016/j.ejmech.2018.09.047

Reference: EJMECH 10758

To appear in: *European Journal of Medicinal Chemistry*

Received Date: 19 May 2018

Revised Date: 21 August 2018

Accepted Date: 14 September 2018

Please cite this article as: T. Han, Y. Wang, M. Wang, X. Li, K. Cheng, X. Gao, Z. Li, J. Bai, H. Hua, D. Li, Synthesis of scutellarein derivatives with antiproliferative activity and selectivity through the intrinsic pathway, *European Journal of Medicinal Chemistry* (2018), doi: https://doi.org/10.1016/j.ejmech.2018.09.047.

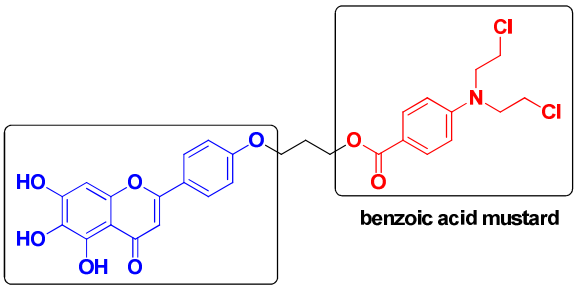

scutellarein

benzoic acid mustard

10a

MCF-7: IC_{50} = 1.5 μM

L-O2: IC_{50} > 50 μM

- Cell cycle arrest at the G1 phase
- MCF-7 cells apoptosis
- MMP ($\Delta\psi_m$) ↓
- Mitochondria-dependent apoptotic pathway

Synthesis of scutellarein derivatives with antiproliferative activity and selectivity through the intrinsic pathway

Tong Han[a], Yan Wang[b], Mingying Wang[a], Xu Li[c], Keguang Cheng[d], Xiang Gao[a], Zhanlin Li[a], Jiao Bai[a], Huiming Hua[a], Dahong Li[a,*]

[a]*Key Laboratory of Structure-Based Drug Design & Discovery, Ministry of Education, and School of Traditional Chinese Materia Medica, Shenyang Pharmaceutical University, 103 Wenhua Road, Shenyang 110016, PR China*

[b]*Yantai Valiant Pharmaceutical Co., Ltd., 60 Taiyuan Road, Dajijia Industrial Park, YEDA Yantai 264006, P. R. China*

[c]*Jiangsu Kanion Pharmaceutical Co., Ltd., 58 Kangyuan Road, Lianyungang 222001, PR China*

[d]*State Key Laboratory for the Chemistry and Molecular Engineering of Medicinal Resources, and School of Chemistry and Pharmacy, Guangxi Normal University, 15 Yucai Raod, Guilin 541004, PR China*

[*]Corresponding author. E-mail addresses: lidahong0203@163.com (D. Li).

ABSTRACT

To explore antitumor agents with potent efficacy and low toxicity, scutellarein derivatives with benzoic acid mustard (**10a**−**c**, **11a**−**c** and **13a**−**c**) were designed and synthesized. The antiproliferative activities of the target derivatives against A549, MCF-7 and Bel-7402 cancer cell lines were tested. Compound **10a** showed the strongest potency with an IC_{50} value of 1.50 μM against MCF-7 cell line, and displayed low toxicity against human liver L-O2 normal cells (IC_{50} > 50 μM), showing specificity between normal and malignant cells. The mechanism studies revealed that **10a** could induce apoptosis in MCF-7 cells, arrest MCF-7 cell cycle at the G1 phase and cause mitochondrial dysfunction in a concentration-dependant manner. Furthermore, the enhanced expression of the pro-apoptotic proteins caspase-9, caspase-3, Bax and cytochrome *c*, and the reduced expression of the anti-apoptotic protein Bcl-2 confirmed that **10a** induced the intrinsic apoptosis pathway in MCF-7 cells. The potent antiproliferative activity and good selectivity guaranteed **10a** a lead compound for the further development into anticancer theraputics, especially for breast cancer.

Keywords: scutellarein, benzoic acid mustard, antiproliferative activity, selectivity

1. Introduction

Cancer is the second cause of mortality worldwide and continuing to be a serious health problem in developing countries [1,2]. According to the data of China, the incidence and mortality of cancer have been increasing. This situation will become more severe with the rapid population aging process in the future [3]. Current studies show that chemotherapy is still the most efficacious cancer treatment approach. However, side effects seriously impede its clinical application [4,5]. Therefore, new drugs which can cause tumor cell death without obvious side effects are of great importances for cancer chemotherapy.

At present, many antitumor compounds have the potentials to alkylate RNA, DNA and several proteins [6]. Among which, classic DNA alkylating agents nitrogen mustards with the advantages of strong potency and broad spectrum have been extensively used [7]. However, the lack of specific affinity for tumor cells necessitates large doses to achieve certain local concentrations, leading to side effects and systemic toxicity [8]. Structural modifications of nitrogen mustards have been done during the last decades in order to overcome these deficiencies. In this regard, changing the combined parts is one of the most effective methods, such as benzene derivatives [9,10], polyamine [11], distamycin [12], steroids [13,14], diterpenoids [15,16], macrolide [17] and so forth. Some achieved good results, especially the hybrids of nitrogen mustards and nature products, such as oridonin (A) [15], glutathione (B) [18], enmein (C) [16] and brefeldin A (D) [17], which exhibited significant antitumor activities and low toxicity (Figure 1). This fact prompts us to explore new carriers from other natural skeletons to obtain nitrogen mustard derivatives with improved selectivity and low toxicity.

Flavonoids, one of the most common classes of naturally occurring phenolic

phytochemicals, have drawn tremendous attention because of their various benficial biological activities and low toxicity [19]. Scutellarin, the main effective flavonoid component of *Erigeron breviscapus (vant.)* Hand-Mazz extract breviscapine [20], has the potency to treat cardiovascular diseases [21−24]. It could also induce apoptosis [25], suppress the migration and invasion [26,27] and sensitize cancer cells to chemotherapy [28,29]. Scutellarein is one of the main metabolites of scutellarin in vivo after breviscapine administration and possesses some similar therapeutic effects as scutellarin [30]. Some recent researches have focused on the anticancer activity of scutellarein [31−38]. Scutellarein was also found to show non-toxic under the long administration duration and/or high dose [39]. These results suggest that scutellarein would be a promising carrier of nitrogen mustards for the discovery of new anticancer agents.

Some nature products and benzoic acid mustard hybrids showed significant antiproliferative activities and benzoic acid mustard was reported to show low toxicity [40,41]. Therefore, in this study, scutellarein and its two analogues were selected to combine with benzoic acid mustard. The target hybrids were evaluated against human tumor A549, Bel-7402 and MCF-7 cells and L-O2 normal hepetic cells for the antiproliferative activities. Further mechanism study concerning apoptosis related properties were also investigated.

2. Result and Discussion

2.1. Chemistry

The synthetic methods of target derivatives **10a**−**c**, **11a**−**c** and **13a**−**c** are shown in Scheme 1. According to the literature [15], **2** was reacted with ethylene oxide in acetic solution to give **3**. Benzoic acid mustard **4** was obtained by the sequences of reaction

of **3** and phosphorus oxychloride, and hydrolysis by using concentrated hydrochloric acid. Treatment of scutellarin **1** with 6 N HCl in ethanol under reflux, scutellarein **5** was synthesized. **6** was got from **2** by the treatment with dichlorodiphenylmethane [42]. **7** was synthesized by the reaction of **5** and 1,2-dibromoethane.

Compounds **8a**−**c** and **12a**−**c** were synthesized in good yields by the reaction of intermediate **6** or **7** with corresponding dibromoalkane in anhydrous acetone, and then converted to **9a**−**c** and **13a**−**c** by the reaction with **4** and K_2CO_3 in anhydrous DMF. **10a**−**c** was obtained by removing the diphenylmethylene ketal of **9a**−**c** with HOAc solution. The reaction of **10a**−**c** with Me_2SO_4 in anhydrous acetone provided **11a**−**c**. NMR (^1H and ^{13}C) and HRMS (high resolution mass spectrum) were used to confirm the structures.

2.2. Biological evaluation

2.2.1 Antiproliferative activity

The antiproliferative activities of **10a**−**c**, **11a**−**c** and **13a**−**c** against three human cancer cell lines MCF-7 (breast cancer), A549 (lung cancer) and Bel-7402 (hepatocellular carcinoma), and normal cells L-O2 (liver) were tested and compared with scutellarein (**2**), benzoic acid mustard (**4**), chlorambucil and positive control 5-FU (5-fluorouracil) in each panel (Table 1). Some derivatives showed antiproliferative activities against tumor cells to some extent and low toxicity against L-O2 nomal cells with IC_{50} values greater than 50 μM, exhibiting selectivity. Among them, **10a**−**c** exhibited stronger antiproliferative activities against MCF-7 and Bel-7402 cells with IC_{50} values between 1.50 and 9.07 μM. **10b** and **10c** displayed moderate activities against A549 cell line with IC_{50} values of 21.47 and 23.51 μM, respectively. While, **11a**−**c**, **13b** and **13c** showed weak antiproliferative activities against Bel-7402 cell line with IC_{50} values ranging from 25.69 to 45.72 μM. The

results that hybrids **10a−c** showed more potent antiproliferative activities than **11a−c** and **13a−c** indicated the unsubstituted 6-OH and 7-OH were beneficial to the antiproliferative activities. The length of the linkers does not seem to regularly affect activities. In particular, **10a−c** also exhibited more potent inhibitory activities with IC_{50} values of 1.50−4.78 μM than benzoic acid mustard (IC_{50} > 50 μM), scutellarein (IC_{50} > 50 μM), chlorambucil (IC_{50} > 50 μM) and 5-FU (IC_{50} 27.89 μM) against MCF-7 cells. Especially, **10a** showed the smallest IC_{50} value of 1.50 μM. Consequently, **10a** was selected for further investigation of the possible cellular mechanisms in MCF-7 cell line.

2.2.2 Cell cycle effect

To determine the effects of **10a** on the cell cycle arrest, MCF-7 cells were treated with certain concentrations of **10a** (0.75, 1.5 and 3 μM) for 48 h and stained with PI (propidium iodide). The DNA content of cell nuclei was analyzed by flow cytometry with non-treated cells as control. G1 phase cells increased from 41.49% (control group) to 44.16%, 50.99% and 59.49% (Figure 2) in a concentration-dependent manner. The results revealed that **10a** caused G1 phase arrest of MCF-7 cells in a concentration-dependent manner.

2.2.3 Cell apoptosis effect

Annexin V-FITC/PI binding assay was carried out to evaluate the apoptosis inducing effects of **10a**. MCF-7 cells were treated with the same concentrations of **10a** as the cell cycle test for 48 h. Then, the annexin-V and PI were used to dyeing cells, and the percentages of apoptotic cells were determined by flow cytometry. The result were given in Figure 3, the apoptosis of MCF-7 cells treated with **10a** increased from 15.99% to 29.31% and 65.21% at the concentrations of 0.75, 1.5 and 3 μM, respectively, compared to 6.09% in the control group. The results proved that **10a**

caused remarkable apoptosis of MCF-7 cells in a concentration-dependent manner.

2.2.4 Mitochondria membrane potential analysis

Mitochondria plays a key role in the induction of apoptosis. The dissipation of mitochondria membrane potential is an significant early event in apoptosis, and then some pro-apoptotic factors such as cytochrome *c*, Bax were released [42,43]. Thus, the effects of **10a** on mitochondrial membrane potentials in MCF-7 cell line were investigated. MCF-7 cells were treated with the same concentrations of **10a** as the cell cycle test for 48 h, and stained with the dye JC-1, the changes of mitochondrial membrane potentials were monitored by flow cytometry. As shown in Figure 4, **10a** induced a concentration-dependent increase in depolarized cell population from 1.61% of control to 19.61%, 43.48% and 64.80%, respectively. This result illustrated that compound **10a** could induced MCF-7 cell apoptosis through mitochondrial (intrinsic) pathways.

2.2.5 Effects on apoptosis-related proteins

The mitochondria-dependent apoptotic pathway is regulated by the Bcl-2 family of pro- and anti-apoptotic proteins such as Bax (pro-apoptotic protein) and Bcl-2 (anti-apoptotic protein), which could induce cytochrome c released into the cytosol, resulting in the activation of the caspase-9 and -3, finally triggering the execution of apoptosis [44,45]. Therefore, to determine compound **10a** involved in the mitochondria-dependent apoptosis pathway in MCF-7 cells, we examined the expression of Bcl-2 and Bax, cyto-*c*, caspase-9 and -3 activities by Western blot analysis. As shown in Figure 5, in comparison with the control cells, **10a** could up-regulation the level of pro-apoptotic protein Bax and down-regulation the level of anti-apoptotic protein Bcl-2 in a dose-dependent fashion. Moreover, the expression of cytochrome c remarkably increased with the elevation of **10a** concentration, this is

probably due to the release from mitochondria (Figure 5). Then, the caspase-9 was activated, which further increased the level of caspase-3 compared to the control in MCF-7 cells. These results indicated that **10a** could induced cell apoptosis via increased the Bax/Bcl-2 ratio, leading to the release of cyto-*c*, caspase-9 and -3 activation, which triggered the execution of apoptosis.

3. Conclusion

In summary, a series of hybrids of scutellarein and benzoic acid mustard were synthesized and evaluated. Some of them showed strong antiproliferative activities against MCF-7 and Bel-7402 cancer cell lines and weak activities against L-O2 human normal liver cells. Among them, compound **10a** exhibited the strongest antiproliferative potency against MCF-7 cell line with an IC_{50} value of 1.50 μM. **10a** also displayed no obvious inhibitory effects against L-O2 cells. In addition, compound **10a** was found to induce apoptosis, G1 phase arrest, and collapse of mitochondrial membrane in a concentration-dependent manner in MCF-7 cells. Therefore, mitochondria-dependent apoptotic pathway would be involved in **10a** mediated apoptosis. Western blot assays indicated that **10a** induced the expression of Bax, cyto-*c*, caspase-9 and -3, while suppressed the expression of Bcl-2. In conclusion, compound **10a** could be considered as a promising anticancer agent and further evaluation of **10a** is on-going.

4. Experimental

4.1. Chemistry

Chemicals and solvents were purchased from commercial sources. Further purification by standard methods were employed when necessary. ^{1}H NMR and ^{13}C

NMR spectra were recorded on a Bruker ARX-400 NMR spectrometer in the indicated solvents (TMS as internal standard): the values of the chemical shifts were expressed in δ values (ppm) and the coupling constants (*J*) in Hz. HRESIMS data were obtained using Bruker micro-TOFQ-Q mass spectrometer.

*4.1.2 General procedures to synthesize **10a−c**, **11a−c** and **13a−c***

To a solution of **6** (450 mg, 1 mmol) in 20 mL of anhydrous acetone, corresponding dibromoalkane (3 mmol) and K_2CO_3 (417 mg, 3 mmol) were added. Followed by refluxing for 12 h and vacuum filtration. This procedure yielded concentrated filter liquor, from which a yellow solid **8a−c** was obtained. **8a−c** (0.3 mmol) in 5 mL of DMF was mixed with benzoic acid mustard **4** (0.35 mmol) and K_2CO_3 (0.6 mmol) by stirring at room temperature for 24 h. The mixture was poured into 20 mL of H_2O and extracted with ethyl acetate (15 mL × 3). The organic layers were combined, washed with water and saturated NaCl solution, dried over anhydrous Na_2SO_4, and concentrated in vacuo, sequentially. The crude material **9a−c** was obtained. Without further purification, **9a−c** was dissolved in 10 mL of HOAc/H_2O (4:1) solution, then refluxed under N_2 atmosphere for 1.5 h. After being cooled down to the room temperature, the mixture was poured into 50 mL water, extracted with ethyl acetate (20 mL × 3), then the organic layer was washed with saturated NaCl solution, dried over Na_2SO_4, filtered and concentrated. The residues were purified by column chromatography (dichloromethane/methanol 20:1) to yield **10a−c**.

K_2CO_3 (0.4 mmol) and Me_2SO_4 (0.4 mmol) were added to a solution of **10a−c** (0.09 mmol) in anhydrous acetone (20 mL). The solution was refluxed for 8 h and filtered in vacuum. The filter liquor was concentrated to obtain a yellow solid. The residues were purified by column chromatography (petroleum ether/ethyl acetate 4:1) to yield **11a−c**. **13a−c** were prepared by a similar procedure as **10a−c**.

4.1.1.1 Compound ***10a****. 3-(4-(5,6,7-trihydroxy-4-oxo-4H-chromen-2-yl)phenoxy) propyl-4-(bis(2-chloroethyl)amino)benzoate*. Yellow power, 85 mg; yield: 41%; HRMS (ESI) *m/z* calcd for $C_{29}H_{27}Cl_2NO_8$ $[M + H]^+$ 588.1147, found 588.1164; ^1H NMR (DMSO-d_6, 400 MHz) δ (ppm): 12.35 (s, 1H, 5-OH), 10.48 (s, 1H, 7-OH), 8.81 (s, 1H, 6-OH), 8.12 (d, 2H, *J* = 8.9 Hz, H-2′,6′), 7.80 (d, 2H, *J* = 8.9 Hz, Ar-H), 7.14 (d, 2H, *J* = 8.9 Hz, Ar-H), 6.83 (d, 3H, *J* = 8.9 Hz, H-3′,5′, H-8), 6.27 (s, 1H, H-3), 4.37 (t, 2H, *J* = 6.2 Hz, -CH_2-), 4.24 (t, 2H, *J* = 6.2 Hz, -CH_2-), 3.76−3.81 (m, 8H, -CH_2-), 2.18 (m, 2H, -CH_2-). ^{13}C NMR (DMSO-d_6, 100 MHz) δ (ppm): 182.59, 166.10, 164.28, 163.54, 161.99, 153.53, 150.77, 145.95, 131.74, 131.63, 131.63, 128.96, 128.96, 123.56, 117.64, 115.42, 115.42, 111.62, 111.62, 103.80, 103.50, 99.15, 65.36, 61.25, 52.17, 52.17, 41.31, 41.31, 28.66.

4.1.1.2 Compound ***10b****, 4-(4-(5,6,7-trihydroxy-4-oxo-4H-chromen-2-yl)phenoxy)butyl 4-(bis(2-chloroethyl)amino)benzoate*. Yellow power, 46 mg; yield: 25%; HRMS (ESI) *m/z* calcd for $C_{30}H_{29}Cl_2NO_8$ $[M + H]^+$ 602.1304, found 602.1339; ^1H NMR (DMSO-d_6, 400 MHz) δ (ppm): 12.76 (s, 1H, 5-OH), 10.38 (s, 1H, 7-OH), 8.82 (s, 1H, 6-OH), 8.01 (d, 2H, *J* = 8.8 Hz, H-2′,6′), 7.77 (d, 2H, *J* = 9.0 Hz, Ar-H), 7.09 (d, 2H, *J* = 9.0 Hz, Ar-H), 6.82 (s, 1H, H-8), 6.79 (d, 2H, *J* = 8.8 Hz, H-3′,5′), 6.60 (s, 1H, H-3), 4.27 (s, 2H, -CH_2-), 4.15 (s, 2H, -CH_2-), 3.74−3.79 (m, 8H, -CH_2-), 1.87 (s, 4H, -CH_2-). ^{13}C NMR (DMSO-d_6, 100 MHz) δ (ppm): 182.50, 166.10, 163.51, 161.98, 153.84, 150.70, 150.16, 147.49, 131.54, 131.54, 131.44, 128.64, 128.64, 123.46, 117.76, 115.47, 115.47, 111.58, 111.58, 104.52, 103.33, 94.37, 67.94, 64.00, 52.15, 52.15, 41.28, 41.28, 25.82, 25.52.

4.1.1.3 Compound ***10c****. 5-(4-(5,6,7-trihydroxy-4-oxo-4H-chromen-2-yl)phenoxy) pentyl-4-(bis(2-chloroethyl)amino)benzoate*. Yellow power, 61 mg; yield: 33%; HRMS (ESI) *m/z* calcd for $C_{31}H_{31}Cl_2NO_8$ $[M + H]^+$ 616.1460, found 616.1496; ^1H

NMR (DMSO-d_6, 400 MHz) δ (ppm): 12.76 (s, 1H, 5-OH), 10.34 (s, 1H, 7-OH), 8.91 (s, 1H, 6-OH), 8.00 (d, 2H, J = 8.8 Hz, H-2′,6′), 7.78 (d, 2H, J = 9.0 Hz, Ar-H), 7.09 (d, 2H, J = 9.0 Hz, Ar-H), 6.82 (t, 3H, J = 8.8 Hz, H-3′,5′, H-8), 6.59 (s, 1H, H-3), 4.23 (t, 2H, J = 6.1 Hz, -CH_2-), 4.09 (t, 2H, J = 6.3 Hz, -CH_2-), 3.75−3.80 (m, 8H, -CH_2-), 1.83−1.74 (m, 4H, -CH_2-), 1.56 (m, 2H, -CH_2-). ^{13}C NMR (DMSO-d_6, 100 MHz) δ (ppm): 182.50, 166.14, 163.53, 162.07, 153.85, 150.71, 150.16, 147.49, 131.53, 131.53, 131.43, 128.64, 128.64, 123.42, 117.84, 115.45, 115.45, 111.61, 111.61, 104.51, 103.32, 94.37, 68.19, 64.13, 52.18, 52.18, 41.31, 41.31, 28.62, 28.49, 22.59.

4.1.1.4 Compound ***11a***. *3-(4-(5-hydroxy-6,7-dimethoxy-4-oxo-4H-chromen-2-yl) phenoxy)propyl-4-(bis(2-chloroethyl)amino)benzoate*. Yellow power, 37 mg; yield: 60%; HRMS (ESI) *m/z* calcd for $C_{31}H_{31}Cl_2NO_8$ $[M + H]^+$ 616.1460, found 616.1452; ^{1}H NMR (DMSO-d_6, 400 MHz) δ (ppm): 12.73 (s, 1H, 5-OH), 8.02 (d, 2H, J = 8.9 Hz, H-2′,6′), 7.80 (d, 2H, J = 8.9 Hz, Ar-H), 7.16 (d, 2H, J = 8.9 Hz, Ar-H), 6.91 (s, 1H, H-8), 6.82 (d, 2H, J = 8.9 Hz, H-3′,5′), 6.59 (s, 1H, H-3), 4.37 (t, 2H, J = 6.0 Hz, -CH_2-), 4.24 (t, 2H, J = 6.2 Hz, -CH_2-), 3.91 (s, 1H, -OCH_3), 3.83 (s, 1H, -OCH_3), 3.73−3.80 (m, 8H, -CH_2-), 2.18 (m, 2H, -CH_2-). ^{13}C NMR (DMSO-d_6, 100 MHz) δ (ppm): 182.65, 166.11, 163.95, 162.18, 158.88, 153.14, 150.78, 149.23, 131.63, 131.63, 128.95, 128.77, 128.77, 123.35, 117.63, 115.66, 115.66, 111.62, 111.62, 104.39, 103.82, 96.48, 65.43, 62.59, 61.59, 56.97, 53.30, 53.30, 41.33, 41.33, 28.63.

4.1.1.5 Compound ***11b***. *4-(4-(5-hydroxy-6,7-dimethoxy-4-oxo-4H-chromen-2-yl) phenoxy)butyl-4-(bis(2-chloroethyl)amino)benzoate*. Yellow power, 21 mg; yield: 43%; HRMS (ESI) *m/z* calcd for $C_{32}H_{33}Cl_2NO_8$ $[M + H]^+$ 630.1617, found 630.1673; ^{1}H NMR (DMSO-d_6, 400 MHz) δ (ppm): 12.74 (s, 1H, 5-OH), 8.02 (d, 2H, J = 8.6 Hz, H-2′,6′), 7.77 (d, 2H, J = 8.9 Hz, Ar-H), 7.14 (d, 2H, J = 8.9 Hz, Ar-H), 6.91 (s, 1H,

H-8), 6.80 (d, 2H, *J* = 9.0 Hz, H-3′,5′), 6.58 (s, 1H, H-3), 4.27 (s, 2H, -CH_2-), 4.15 (s, 2H, -CH_2-), 3.91 (s, 1H, -OCH_3), 3.83 (s, 1H, -OCH_3), 3.74−3.78 (m, 8H, -CH_2-), 1.87 (s, 4H, -CH_2-). ^{13}C NMR (DMSO-d_6, 100 MHz) δ (ppm): 182.65, 166.10, 163.95, 162.27, 158.86, 157.13, 150.70, 149.22, 131.98, 131.53, 131.53, 128.72, 128.72, 123.20, 117.77, 115.64, 115.64, 111.57, 111.57, 104.39, 103.76, 96.47, 67.99, 63.98, 61.57, 56.96, 52.15, 52.15, 41.27, 41.27, 25.78, 25.52.

4.1.1.6 Compound ***11c****. 5-(4-(5-hydroxy-6,7-dimethoxy-4-oxo-4H-chromen-2-yl) phenoxy)pentyl-4-(bis(2-chloroethyl)amino)benzoate*. Yellow power, 34 mg; yield: 53%; HRMS (ESI) *m/z* calcd for $C_{33}H_{35}Cl_2NO_8$ $[M + H]^+$ 644.1773, found 644.1635; ^{1}H NMR (DMSO-d_6, 400 MHz) δ (ppm): 12.75 (s, 1H, 5-OH), 8.05 (d, 2H, *J* = 8.9 Hz, H-2′,6′), 7.78 (d, 2H, *J* = 8.9 Hz, Ar-H), 7.14 (d, 2H, *J* = 8.9 Hz, Ar-H), 6.92 (s, 1H, H-8), 6.81 (d, 2H, *J* = 8.9 Hz, H-3′,5′), 6.59 (s, 1H, H-3), 4.24 (s, 2H, -CH_2-), 4.11 (s, 2H, -CH_2-), 3.92 (s, 1H, -OCH_3), 3.83 (s, 1H, -OCH_3), 3.75−3.80 (m, 8H, -CH_2-), 1.72−1.85 (m, 4H, -CH_2-), 1.56 (m, 2H, -CH_2-). ^{13}C NMR (DMSO-d_6, 100 MHz) δ (ppm): 182.66, 166.13, 164.01, 162.38, 158.88, 157.14, 150.71, 149.24, 131.53, 131.53, 128.74, 128.74, 123.17, 117.84, 115.65, 115.65, 111.61, 111.61, 104.39, 103.76, 96.49, 68.27, 64.14, 61.59, 56.97, 52.17, 52.17, 41.31, 41.31, 28.61, 28.50, 22.60.

4.1.1.7 Compound ***13a****. 3-(4-(10-hydroxy-9-oxo-2,3-dihydro-9H-[1,4]dioxino[2,3-g] chromen-7-yl)phenoxy)propyl-4-(bis(2-chloroethyl)amino)benzoate.* Yellow power, 13 mg; yield: 36%; HRMS (ESI) *m/z* calcd for $C_{31}H_{29}Cl_2NO_8$ $[M + H]^+$ 614.1304, found 614.1364; ^{1}H NMR (DMSO-d_6, 400 MHz) δ (ppm): ^{1}H NMR (DMSO-d_6, 400 MHz) δ (ppm): 12.32 (s, 1H, 5-OH), 8.00 (d, 2H, *J* = 8.9 Hz, H-2′,6′), 7.79 (d, 2H, *J* = 8.9 Hz, Ar-H), 7.14 (d, 2H, *J* = 8.9 Hz, Ar-H), 6.94 (s, 1H, H-8), 6.80 (d, 2H, *J* = 8.9 Hz, H-3′,5′), 6.33 (s, 1H, H-3), 4.42−4.30 (m, 6H, -CH_2-), 4.23 (m, 2H, -CH_2-), 3.76−3.80

(m, 8H, -CH_2-), 2.19 (m, 2H, -CH_2-). ^{13}C NMR (DMSO-d_6, 100 MHz) δ (ppm): 182.48, 166.10, 163.63, 162.16, 153.49, 150.77, 150.42, 145.05, 131.73, 131.63, 131.63, 128.69, 128.69, 123.19, 117.65, 115.60, 115.60, 111.48, 111.48, 105.26, 104.19, 99.52, 65.63, 65.42, 64.29, 61.25, 52.24, 52.24, 41.31, 41.31, 28.64.

4.1.1.8 Compound ***13b***. *4-(4-(10-hydroxy-9-oxo-2,3-dihydro-9H-[1,4]dioxino[2,3-g] chromen-7-yl)phenoxy)butyl 4-(bis(2-chloroethyl)amino)benzoate*. Yellow power, 21 mg; yield: 44%; HRMS (ESI) *m/z* calcd for $C_{32}H_{31}Cl_2NO_8$ $[M + H]^+$ 628.1460, found 628.1462; ^{1}H NMR (DMSO-d_6, 400 MHz) δ (ppm): 12.32 (s, 1H, 5-OH), 7.99 (d, 2H, *J* = 8.9 Hz, H-2′,6′), 7.77 (d, 2H, *J* = 8.9 Hz, Ar-H), 7.13 (d, 2H, *J* = 8.9 Hz, Ar-H), 6.93 (s, 1H, H-8), 6.79 (d, 2H, *J* = 8.9 Hz, H-3′,5′), 6.33 (s, 1H, H-3), 4.42 (s, 2H, -CH_2-), 4.38 (s, 2H, -CH_2-), 4.28 (s, 2H, -CH_2-), 4.15 (s, 2H, -CH_2-), 3.74−3.78 (m, 8H, -CH_2-), 1.87 (s, 2H, -CH_2-). ^{13}C NMR (DMSO-d_6, 100 MHz) δ (ppm): 182.48, 166.10, 163.67, 162.27, 153.50, 150.70, 150.42, 149.68, 131.73, 131.53, 131.53, 128.66, 128.66, 123.04, 117.78, 115.60, 115.60, 111.58, 111.58, 105.27, 104.13, 99.52, 67.99, 65.64, 64.30, 64.00, 52.16, 52.16, 41.27, 41.27, 25.81, 25.52.

4.1.1.9 Compound ***13c***. *5-(4-(10-hydroxy-9-oxo-2,3-dihydro-9H-[1,4]dioxino[2,3-g] chromen-7-yl)phenoxy)pentyl 4-(bis(2-chloroethyl)amino)benzoate*. Yellow power, 34 mg; yield: 53%; HRMS (ESI) *m/z* calcd for $C_{33}H_{33}Cl_2NO_8$ $[M + H]^+$ 642.1617, found 642.1695; ^{1}H NMR (DMSO-d_6, 400 MHz) δ (ppm): 12.32 (s, 1H, 5-OH), 7.98 (d, 2H, *J* = 8.9 Hz, H-2′,6′), 7.78 (d, 2H, *J* = 9.0 Hz, Ar-H), 7.11 (d, 2H, *J* = 9.0 Hz, Ar-H), 6.92 (s, 1H, H-8), 6.81 (d, 2H, *J* = 8.9 Hz, H-3′,5′), 6.32 (s, 1H, H-3), 4.42 (d, 2H, *J* = 4.5 Hz, -CH_2-), 4.38 (d, 2H, *J* = 4.7 Hz, -CH_2-), 4.23 (t, 2H, *J* = 6.2 Hz, -CH_2-), 4.08 (t, 2H, *J* = 6.3 Hz, -CH_2-), 3.80−3.75 (m, 8H, -CH_2-), 1.82−1.73 (m, 4H, -CH_2-), 1.55 (m, 2H, -CH_2-). ^{13}C NMR (DMSO-d_6, 100 MHz) δ (ppm): 182.45, 166.12, 163.65, 162.33, 153.48, 150.68, 150.41, 149.65, 131.73, 131.53, 131.53, 128.64, 128.64,

122.97 117.83, 115.53, 115.53, 111.58, 111.58, 105.24, 104.08, 99.50, 68.22, 65.62, 64.28, 64.13, 52.17, 52.17, 41.29, 41.29, 28.63, 28.51, 22.60.

4.2 MTT assay

The cell viability were assessed by the MTT method. Three cancer cell in logarithmic growth were seeded to each well and incubated for 24 h at 37 ^{o}C in a humidified atmosphere of 5% CO_2. Then target hybrids, scutellarein, benzoic acid mustard and 5-FU were added. 20 μL fresh MTT solution (5 mg/mL) per well was added to each cultured medium after 72 h, and incubated for another 4 h. The cells were dissolved with DMSO (150 μL) and shaken for 10 min at room temperature. After that, the OD of each single well was measured on a Microplate Reader (BIO-RAD) and the IC_{50} values were calculated [46].

4.3 Cell cycle analysis

MCF-7 cells in logarithmic growth were plated in 6-well plates and incubated at 37 ^{o}C for 24 h, then cells were incubated with **10a** at different concentrations (0, 0.75, 1.5 and 3 μM). After 48 h, cells were collected, centrifuged and fixed with 70% ethanol at 4 ^{o}C overnight. The fixed cells were washed with ice-cold PBS and treated with 100 μL RNase A at 37 °C for 30 min, after that stained with 400 μL PI in the dark at 4 °C for 30 min. The cellular DNA content for cycle distribution analysis was performed using a fow cytometer (FACS Calibur Becton–Dickinson) [47].

4.4 Cell apoptosis assay

MCF-7 cells in logarithmic growth were plated in 6-well plates and incubated at 37 ^{o}C for 24 h, then cells were incubated with **10a** at different concentrations (0, 0.75, 1.5 and 3 μM). After 48 h, cells were collected and washed with PBS, then 500 μL binding buffer was added. Finally, double stained Annexin V-FITC/PI (KGA1024, KeyGEN Biotech, Nanjing, China) were added and incubated at room temperature for

15 min in the dark. The cells were detected to analyze apoptosis by fow cytometry [48].

4.5 Mitochondrial membrane potential assay

Briefly, MCF-7 cells in logarithmic growth were plated in 6-well plates and incubated with **10a** at different concentrations (0, 0.75, 1.5 and 3 μM) for 48 h. Cells were collected and washed with PBS. JC-1 dye was used to stained cells under dark conditions according to the manufacturer's instructions (KGA601, KeyGEN Biotech, Nanjing, China). The percentage of cells with collapsed mitochondrial membrane potentials was monitored by flow cytometry [49].

4.6 Western blot assay

MCF-7 cells in logarithmic growth were plated in 6-well plates and incubated with **10a** at different concentrations (0, 0.75, 1.5 and 3 μM) for 48 h, the cells were harvested. Then the cells were lysed using lysis buffer, and the solution was centrifuged at 14000 g for 10 min at 4 ^{o}C. Thereafter, the protein concentrations were determined with bicinchoninic acid protein assay kit (Beyotime Co, Shanghai, China), and individual cell lysates (25 μg) were separated by SDS-PAGE on a 12% polyacrylamide gel and transferred onto nitrocellulose membranes. The membranes were blocked with 5% fat-free milk, the membranes were incubated with monoclonal antibodies against Bcl-2, Bax, cyto-*c*, caspase-9, -3 and GAPDH (KeyGEN Biotech, Nanjing, China) at 4 ^{o}C overnight, respectively. Then, the bound antibodies washed with TBST, and incubated with appropriate second antibodies and followed by enhanced chemiluminescence detection [50].

Acknowledgment

This work was financially supported by the Key Laboratory for the Chemistry and

Molecular Engineering of Medicinal Resources (Guangxi Normal University), the Ministry of Education of China (CMEMR2015-B07), Natural Science Foundation of Liaoning Province (20170540858), General Scientific Research Projects of Department of Education in Liaoning Province (2017LQN05), Key Laboratory of Quality Control of TCM of Liaoning Province (17-137-1-00), and Career Development Support Plan for Young and Middle-aged Teachers in Shenyang Pharmaceutical University.

References

[1] C. Allemani, H.K. Weir, H. Carreira, R. Harewood, D. Spika, X.S. Wang, F. Bannon, J.V. Ahn, C.J. Johnson, A. Bonaventure, R. Marcos-Gragera, C. Stiller, G. Azevedo e Silva, W.Q. Chen, O.J. Ogunbiyi, B. Rachet, M.J. Soeberg, H. You, T. Matsuda, M. Bielska-Lasota, H. Storm, T.C. Tucker, M.P. Coleman, CONCORD Working Group, Global surveillance of cancer survival 1995-2009: analysis of individual data for 25,676,887 patients from 279 population-based registries in 67 countries (CONCORD-2), Lancet 385 (2015) 977−1010.

[2] A.B. Ryerson, C.R. Eheman, S.F. Altekruse, J.W. Ward, A. Jemal, R.L. Sherman, S.J. Henley, D. Holtzman, A. Lake, A.M. Noone, R.N. Anderson, J. Ma, K.N. Ly, K.A. Cronin, L. Penberthy, B.A. Kohler, Annual report to the nation on the status of cancer, 1975−2012, featuring the increasing incidence of liver cancer, Cancer 122 (2016) 1312−1337.

[3] W. Chen, R. Zheng, P.D. Baade, S. Zhang, H. Zeng, F. Bray, A. Jemal, X.Q. Yu, J. He, Cancer statistics in China, 2015, CA-Cancer J. Clin. 66 (2016) 115−132.

[4] W. Derek, J.J. Turchi, Chemotherapy induced DNA damage response, Cancer Biol. Ther. 14 (2013) 379−389.

[5] K. Nurgali, R.T. Jagoe, R. Abalo, Editorial: adverse effects of cancer chemotherapy: Anything new to improve tolerance and reduce sequelae? Front. Pharmacol. 9 (2018) 245.

[6] P. Saha, C. Debnath, G. Bérubé, Steroid-linked nitrogen mustards as potential anticancer therapeutics: A review, J. Steroid Biochem. Mol. Biol. 137 (2013) 271−300.

[7] L.F. Povirk, D.E. Shuker, DNA damage and mutagenesis induced by nitrogen mustards, Mutat. Res. 318 (1994) 205−226.

[8] B.J. Sanderson, A.J Shield, Mutagenic damage to mammalian cells by therapeutic alkylating agents, Mutat. Res. 355 (1996) 41−57.

[9] S. Li, X. Wang, Y. He, M. Zhao, Y. Chen, J. Xu, M. Feng, J. Chang, H. Ning, C. Qi, Design and synthesis of novel quinazoline nitrogen mustard derivatives as potential therapeutic agents for cancer, Eur. J. Med. Chem. 67 (2013) 293−301.

[10] B. Marvania, R. Kakadiya, W. Christian, T.L. Chen, M.H. Wu, S. Suman, K. Tala, T.C. Lee, A. Shah, T.L. Su, The synthesis and biological evaluation of new DNA-directed alkylating agents, phenyl *N*-mustard-4-anilinoquinoline conjugates containing a urea linker, Eur. J. Med. Chem. 83 (2014) 695−708.

[11] P.M. Cullis, L. Merson-Davies, R. Weaver, Conjugation of a polyamine to the bifunctional alkylating agent chlorambucil does not alter the preferred cross-linking site in duplex DNA, J. Am. Chem. Soc. 117 (1995) 8033−8034.

[12] P.G. Baraldi, R. Romagnoli, A.E. Guadix, M.J. de las Infantas Pineda, M.A. Gallo, A. Espinosa, A. Martinez, J.P. Bingham, J.A. Hartley, Design, synthesis, and biological activity of hybrid compounds between uramustine and DNA minor groove binder distamycin A, J. Med. Chem. 45 (2002) 3630−3638.

[13] D. Bastien, R. Hanna, V. Leblanc, É. Asselin, G. Bérubé, Synthesis and

preliminary in vitro biological evaluation of 7α-testosterone-chlorambucil hybrid designed for the treatment of prostate cancer, Eur. J. Med. Chem. 64 (2013) 442−447.

[14] P.C. Acharya, R. Bansal. Synthesis of androstene oxime-nitrogen mustard bioconjugates as potent antineoplastic agents, Steroids 123 (2017) 73−83.

[15] S. Xu, L. Pei, C. Wang, Y.K. Zhang, D. Li, H. Yao, X. Wu, Z.S. Chen, Y. Sun, J. Xu, Novel hybrids of natural oridonin-bearing nitrogen mustards as potential anticancer drug candidates, ACS Med. Chem. Lett. 5 (2014) 797−802.

[16] X. Gao, J. Li, M. Wang, S. Xu, W. Liu, L. Zang, Z. Li, H. Hua, J. Xu, D. Li, Novel enmein-type diterpenoid hybrids coupled with nitrogen mustards: Synthesis of promising candidates for anticancer therapeutics, Eur. J. Med. Chem. 146 (2018) 588−598.

[17] T. Han, K. Tian, H. Pan, Y. Liu, F. Xu, Z. Li, T. Uchita, M. Gao, H. Hua, D. Li, Novel hybrids of brefeldin A and nitrogen mustards with improved antiproliferative selectivity: Design, synthesis and antitumor biological evaluation, Eur. J. Med. Chem. 150 (2018) 53−63.

[18] Y.Z. Xu, X.Y. Gu, S.J. Peng, J.G. Fang, Y.M. Zhang, D.J. Huang, J.J. Chen, K. Gao, Design, synthesis and biological evaluation of novel sesquiterpene mustards as potential anticancer agents, Eur. J. Med. Chem. 94 (2015) 284−297.

[19] M. Singh, M. Kaur, O. Silakari, Flavones: An important scaffold for medicinal chemistry, Eur. J. Med. Chem. 84 (2014) 206−239.

[20] Z.H. Shi, N.G. Li, Z.J. Wang, Y.P. Tang, Z.X. Dong, W. Zhang, P.X. Zhang, T. Gu, W.Y. Wu, J.P. Yang, J.A. Duan, Synthesis and biological evaluation of methylated scutellarein analogs based on metabolic mechanism of scutellarin in vivo, Eur. J. Med. Chem. 106 (2015) 95−105.

[21] X. Chen, X. Shi, X. Zhang, H. Lei, S. Long, H. Su, Z. Pei, R. Huang, Scutellarin

attenuates hypertension-induced expression of brain Toll-like receptor 4/nuclear factor kappa B, Mediators Inflamm. 2013 (2013) 432623.

[22] Z. Pan, W. Zhao, X. Zhang, B. Wang, J. Wang, X. Sun, X. Liu, S. Feng, B. Yang, Y. Lu, Scutellarin alleviates interstitial fibrosis and cardiac dysfunction of infarct rats by inhibiting TGFβ1 expression and activation of p38-MAPK and ERK1/2, Br. J. Pharmacol. 162 (2011) 688−700.

[23] H. Zhou, X. Chen, L. Chen, X. Zhou, G. Zheng, H. Zhang, W. Huang, J. Cai, Anti-fibrosis effect of scutellarin via inhibition of endothelial-mesenchymal transition on isoprenaline-induced myocardial fibrosis in rats, Molecules 19 (2014) 15611−15623.

[24] Z. Wang, J. Yu, J. Wu, F. Qi, H. Wang, Z. Wang, Z. Xu, Scutellarin protects cardiomyocyte ischemia-reperfusion injury by reducing apoptosis and oxidative stress, Life Sci. 157 (2016) 200–207.

[25] Y. Feng, S. Zhang, J. Tu, Z. Cao, Y. Pan, B. Shang, R. Liu, M. Bao, P. Guo, Q. Zhou, Novel function of scutellarin in inhibiting cell proliferation and inducing cell apoptosis of human Burkitt lymphoma Namalwa cells, Leuk. Lymphoma 53 (2012) 2456–2464.

[26] H. Li, H. Fan, Z. Wang, J. Zheng, W. Cao, Potentiation of scutellarin on human tongue carcinoma xenograft by low-intensity ultrasound, Plos One 8 (2013) e59473.

[27] Y. Ke, T. Bao, X. Wu, H. Tang, Y. Wang, J. Ge, B. Fu, X. Meng, L. Chen, C. Zhang, Y. Tan, H. Chen, Z. Guo, F. Ni, X. Lei, Z. Shi, D. Wei, L. Wang, Scutellarin suppresses migration and invasion of human hepatocellular carcinoma by inhibiting the STAT3/Girdin/Akt activity, Biochem. Biophys. Res. Commun. 483 (2017) 509–515.

[28] J.Y. Chan, B.K. Tan, S.C. Lee, Scutellarin sensitizes drug-evoked colon cancer

cell apoptosis through enhanced caspase-6 activation, Anticancer Res. 29 (2009) 3043–3047.

[29] C. Gao, Y. Zhou, Z. Jiang, Y. Zhao, D. Zhang, X. Cong, R. Cao, H. Li, W. Tian, Cytotoxic and chemosensitization effects of scutellarin from traditional Chinese herb *Scutellaria altissima* L. in human prostate cancer cells, Oncol. Rep. 38 (2017) 1491–1499.

[30] Z. Sang, X. Qiang, Y. Li, R. Xu, Z. Cao, Q. Song, T. Wang, X. Zhang, H. Liu, Z. Tan, Y. Deng, Design, synthesis and evaluation of scutellarein-*O*-acetamidoalkylbenzylamines as potential multifunctional agents for the treatment of Alzheimer's disease, Eur. J. Med. Chem. 135 (2017) 307–323.

[31] H. Xu, S. Zhang, Scutellarin-induced apoptosis in HepG2 hepatocellular carcinoma cells via a STAT3 pathway, Phytother. Res. 27 (2013) 1524–1528.

[32] N. Yang, Y. Zhao, Z. Wang, Y. Liu, Y. Zhang, Scutellarin suppresses growth and causes apoptosis of human colorectal cancer cells by regulating the p53 pathway, Mol. Med. Rep. 15 (2017) 929–935.

[33] P. Thirusangu, V. Vigneshwaran, B.R. Vijay Avin, H. Rakesh, H.M. Vikas, B.T. Prabhakar, Scutellarein antagonizes the tumorigenesis by modulating cytokine VEGF mediated neoangiogenesis and DFF-40 actuated nucleosomal degradation, Biochem. Biophys. Res. Commun. 484 (2017) 85.

[34] L. You, H. Zhu, C. Wang, F. Wang, Y. Li, Y. Li Y. Wang, B. He, Scutellarin inhibits Hela cell growth and glycolysis by inhibiting the activity of pyruvate kinase M2, Bioorg. Med. Chem. Lett. 27 (2017) 5404–5408.

[35] D. Goh, Y.H. And, E.S. Ong, Inhibitory effects of a chemically standardized extract from *Scutellaria barbata* in Human colon cancer cell lines, LoVo, J. Agric. Food Chem. 53 (2005) 8197–8204.

[36] X. Shi, G. Chen, X. Liu, Y. Qiu, S. Yang, Y. Zhang, X. Fang, C. Zhang, X. Liu, Scutellarein inhibits cancer cell metastasis in vitro and attenuates the development of fibrosarcoma in vivo, Int. J. Mol. Med. 35 (2015) 31–38.

[37] M. Feng,·Y. Song, J. Wu, X. Chen, Y. Zhang, Study on antitumour activity of scutellarin and its metabolite scutellarein by combining activity screening, target tissue distribution and pharmacokinetics, Chromatographia 80 (2017) 427–435.

[38] F. Guo, F. Yang, Y. Zhu. Scutellarein from *Scutellaria barbata* induces apoptosis of human colon cancer HCT116 cells through the ROS-mediated mitochondria-dependent pathway, Nat. Prod. Res. (2018) https://doi.org/10.1080/14786419. 2018.1440230.

[39] X. Li, L. Wang, Y. Li, L. Bai, M. Xue, Acute and subacute toxicological evaluation of scutellarin in rodents, Regul. Toxicol. Pharmacol. 60 (2011) 106–111..

[40] Q.Z. Zheng, F. Zhang, K. Cheng, Y. Yang, Y. Chen, Y. Qian, H.J. Zhang, H.Q. Li, C.F. Zhou, S.Q. An, Q.C. Jiao, H.L. Zhu, Synthesis, biological evaluation and molecular docking studies of amide-coupled benzoic nitrogen mustard derivatives as potential antitumor agents, Bioorg. Med. Chem. 18 (2010) 880–886.

[41] Z.H. Shi, N.G. Li, Q.P. Shi, W. Zhang, Z.X. Dong, Y.P. Tang, P.X. Zhang, T. Gu, W.Y. Wu, F. Fang, X. Xue, H.M. Li, J.P. Yang, J.A. Duan, Synthesis of scutellarein derivatives to increase biological activity and water solubility, Bioorg. Med. Chem. 23 (2015) 6875–6884.

[42] T.S. Reddy, S.H. Privér, N. Mirzadeh, S.K. Bhargava, Synthesis of gold(I) phosphine complexes containing the 2-$BrC_6F_4PPh_2$ ligand: Evaluation of anticancer activity in 2D and 3D spheroidal models of HeLa cancer cells, Eur. J. Med. Chem. 145 (2018) 291–301.

[43] X. Hu, R. Jiao, H. Li, X. Wang, H. Lyu, X. Gao, F. Xu, Z. Li, H. Hua, D. Li,

Antiproliferative hydrogen sulfide releasing evodiamine derivatives and their apoptosis inducing properties, Eur. J. Med. Chem. 151 (2018) 376–388.

[44] J.F.R. Kerr, A.H. Wyllie, A.R. Currie, Apoptosis: a basic biological phenomenon with wide-ranging implications in tissue kinetics, Br. J. Canc. 26 (1972) 239–257.

[45] G.M. Cohen, Caspases: the executioners of apoptosis, Biochem. J. 326 (1997) 1–16.

[46] J. Chen, T. Wang, S. Xu, P. Zhang, A. Lin, L. Wu, H. Yao, W. Xie, Z. Zhu, J. Xu, Discovery of novel antitumor nitric oxide-donating *β*-elemene hybrids through inhibiting the PI3K/Akt pathway, Eur. J. Med. Chem. 28 (2017) 414–423.

[47] T. Han, J. Li, J. Xue, H. Li, F. Xu, K. Cheng, D. Li, Z. Li, M. Gao, H. Hua, Scutellarin derivatives as apoptosis inducers: Design, synthesis and biological evaluation, Eur. J. Med. Chem. 135 (2017) 270–281.

[48] K. Tian, F. Xu, X. Gao, T. Han, J. Li, H. Pan, L. Zang, D. Li, Z. Li, T. Uchita, M. Gao, H. Hua, Nitric oxide-releasing derivatives of brefeldin A as potent and highly selective anticancer agents, Eur. J. Med. Chem. 136 (2017) 131–143.

[49] J. Chen, T. Wang, S. Xu, A. Lin, H. Yao, W. Xie, Z. Zhu, J. Xu, Design, synthesis and biological evaluation of novel nitric oxide-donating protoberberine derivatives as antitumor agents, Eur. J. Med. Chem. 132 (2017) 173–183.

[50] S. Xu, H. Yao, L. Pei, M. Hu, D. Li, Y. Qiu, G. Wang, L. Wu, H. Yao, Z. Zhu, J. Xu, Design, synthesis, and biological evaluation of NAD(P)H: Quinone oxidoreductase (NQO1)-targeted oridonin prodrugs possessing indolequinone moiety for hypoxia-selective activation, Eur. J. Med. Chem. 132 (2017) 310–321.

Table 1 Antiproliferative activities of target hybrids against different cell lines.

Compound	IC_{50} (μM)[a]			
	A549	MCF-7	Bel-7402	L-O2
10a	> 50	1.50 ± 0.06	7.96 ± 0.45	> 50
10b	21.47 ± 1.26	3.55 ± 0.19	9.07 ± 0.34	> 50
10c	23.51 ± 1.42	4.78 ± 0.31	4.59 ± 0.23	> 50
11a	> 50	> 50	27.83 ± 1.02	> 50
11b	47.28 ± 2.87	> 50	25.69 ± 1.33	> 50
11c	> 50	> 50	32.46 ± 2.30	> 50
13a	44.52 ± 1.90	45.04 ± 2.47	>50	> 50
13b	> 50	> 50	37.64 ± 2.26	> 50
13c	> 50	34.70 ± 1.88	45.72 ± 1.78	> 50
4	> 50	> 50	23.94 ± 1.34	32.86 ± 2.39
scutellarein	> 50	> 50	> 50	> 50
chlorambucil	> 50	> 50	> 50	> 50
5-FU	2.05 ± 0.11	27.89 ± 1.66	18.65 ± 1.31	NT[b]

[a] IC_{50}: concentrations inhibit 50% of cell growth measured by the MTT assay. The values are expressed as average ± standard deviations of three independent experiments. [b] NT: not tested.

1. Legends of Fig. 1, **Fig. 2**, **Fig. 3**, **Fig. 4**, **Fig. 5** and **Scheme 1**

Fig. 1. The chemical structures of some reported natural product/benzoic acid mustard hybrids.

Fig. 2. Cell cycle analysis of **10a** in MCF-7 cells by flow cytometry.

Fig. 3. Flow cytometry analysis of apoptosis induced by **10a** in MCF-7 cells.

Fig. 4. 10a induced mitochondrial depolarization in MCF-7 cells.

Fig. 5. 10a affected the expressions of the mitochondria pathway related proteins in MCF-7 cells. Con is short for control.

Scheme 1. Synthesis of benzoic acid mustard/scutellarein hybrids **10a−c**, **11a−c** and **13a−c**. Reagents and conditions: (a) ethylene oxide, H_2O, CH_3COOH, rt, 24 h; (b) $POCl_3$, 50 ^oC, 0.5 h; (c) 10% HCl, 12 h; (d) HCl, EtOH, N_2, reflux, 36 h; (e) Ph_2CCl_2, Ph_2O, 175 ^oC, 1.5 h; (f) 1,2-dibromoethane, K_2CO_3, DMF, 85 ^oC, 3 h; (g) corresponding dibromoalkane, K_2CO_3, anhydrous acetone, reflux, 6-8 h; (h) **4**, K_2CO_3, anhydrous DMF, rt, 12 h; (i) HAc : H_2O (4:1), reflux, 1.5 h; (j) Me_2SO_4, K_2CO_3, anhydrous acetone, reflux, 8 h; (k) corresponding dibromoalkane, K_2CO_3, anhydrous acetone, reflux, 6-8 h; (l) **4**, K_2CO_3, anhydrous DMF, rt, 12 h.

2. Graphics for Fig. 1, **Fig. 2**, **Fig. 3**, **Fig. 4**, **Fig. 5** and **Scheme 1**

Figure 1

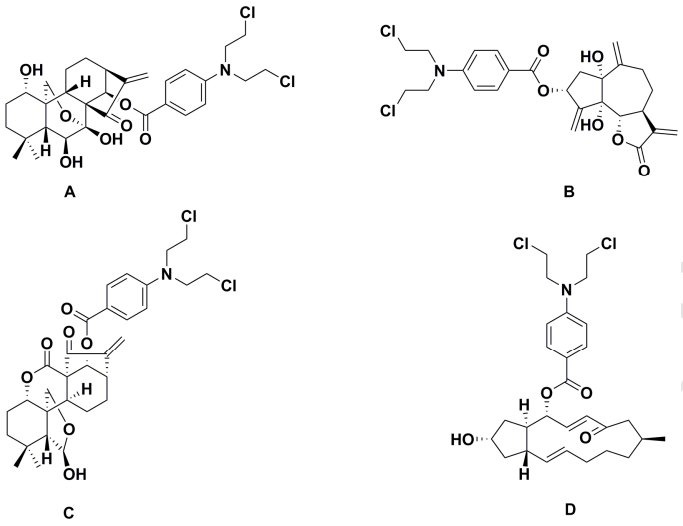

Figure 2

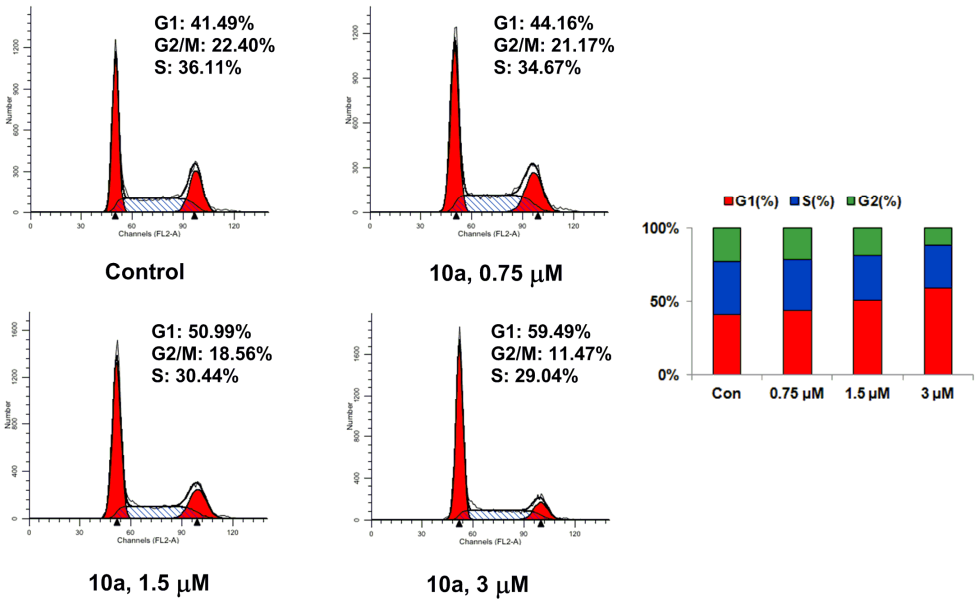

Figure 3

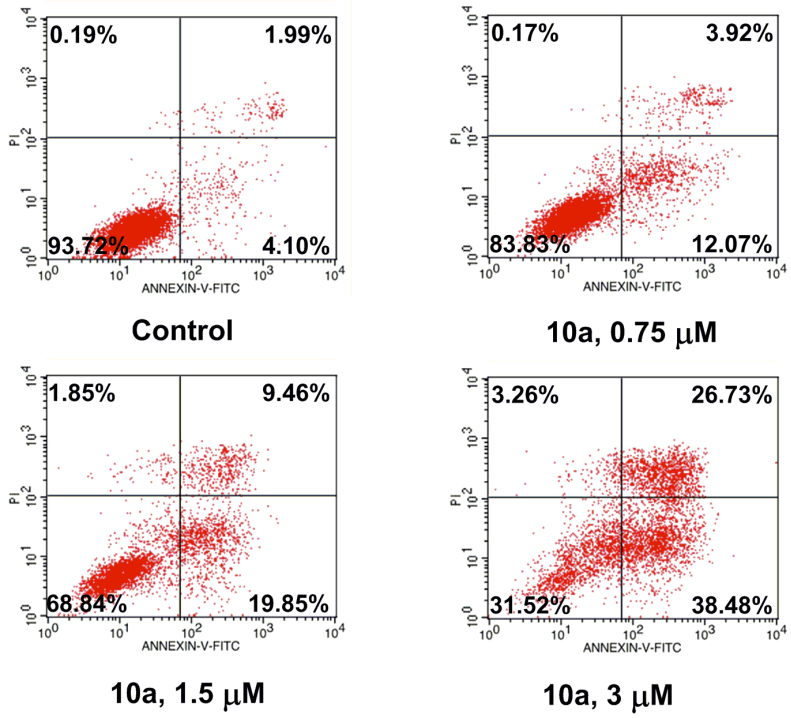

Figure 4

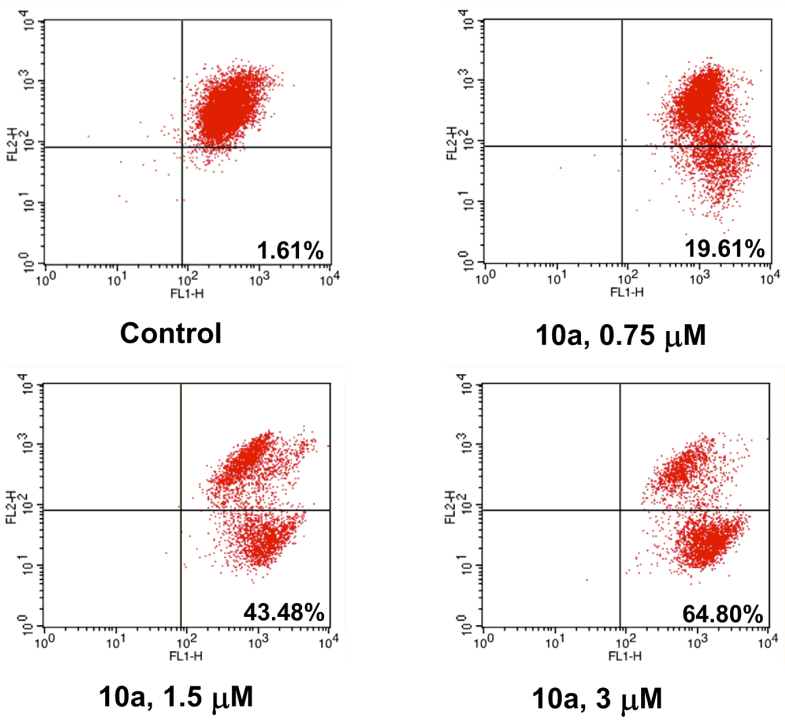

Figure 5

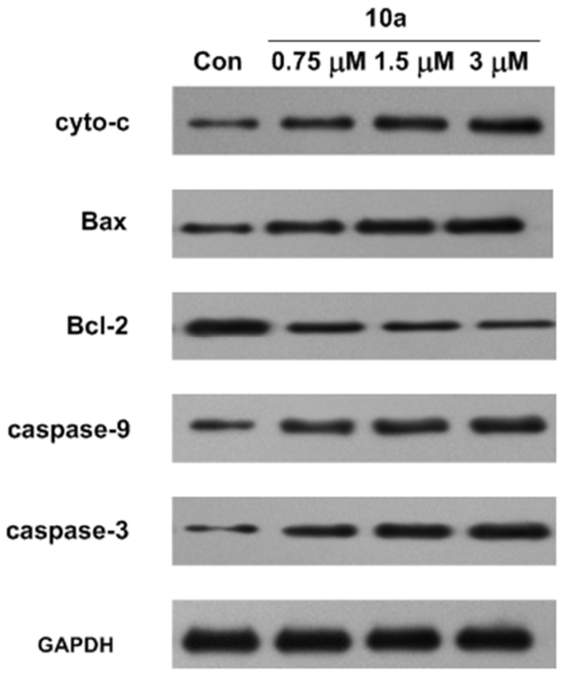

Scheme 1

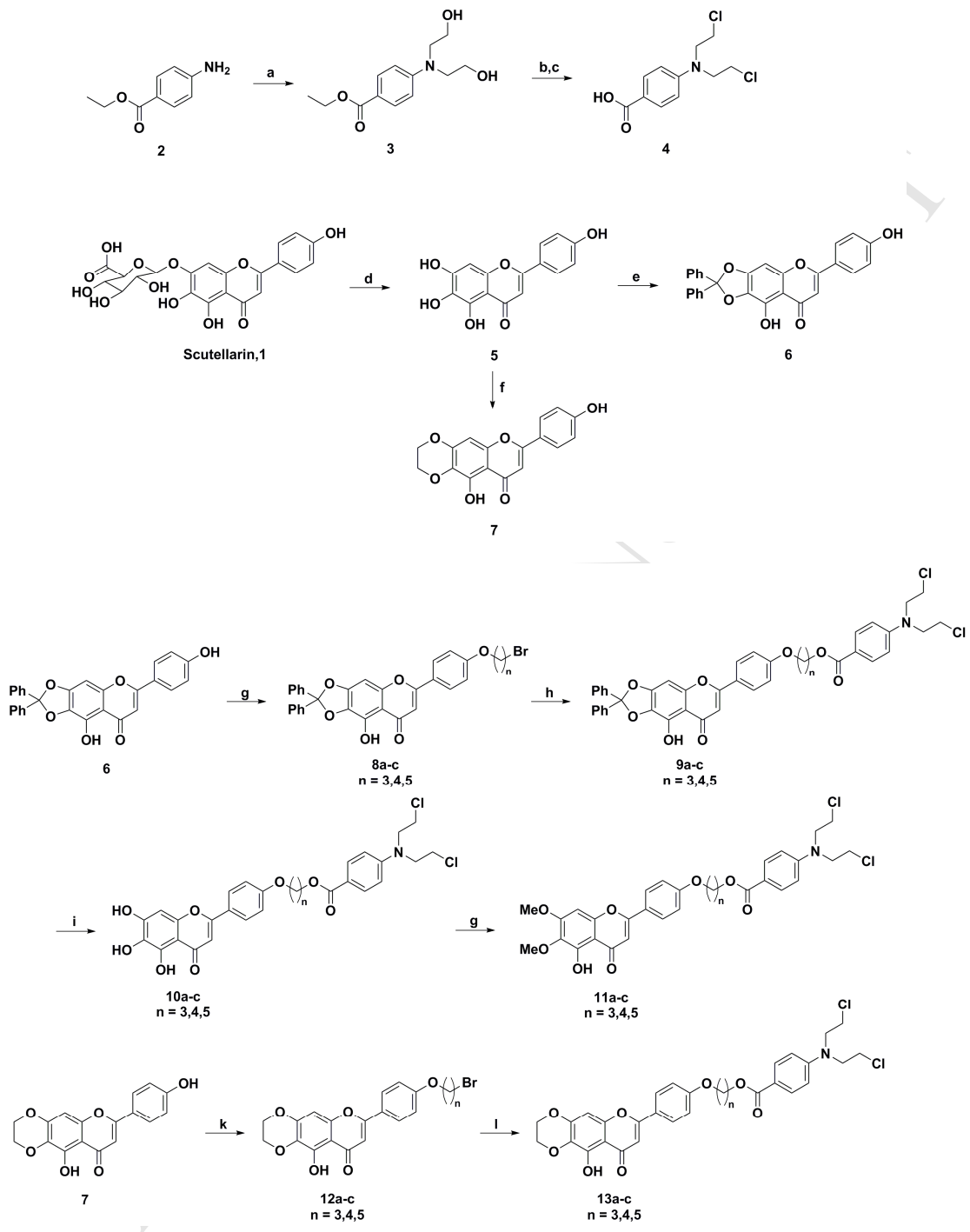
2
3
4
Scutellarin,1
5
6
7
6
8a-c
n = 3,4,5
9a-c
n = 3,4,5
10a-c
n = 3,4,5
11a-c
n = 3,4,5
7
12a-c
n = 3,4,5
13a-c
n = 3,4,5

Highlights

Hybrids of scutellarein and benzoic acid mustard were designed and synthesized.
Some exhibited potent antiproliferative activities with low IC_{50} values.
Compound **10a** showed good selectivity between human normal and tumor cells.
10a induced apoptosis and arrest cell cycle at G1 phase in MCF-7 cells.
10a induced MCF-7 cells apoptosis via the mitochondria-dependent pathways.